A Stochastic Operational Model for Controlling Electric Vehicle Charging to Provide Frequency Regulation

Fei Wu, Ramteen Sioshansi*

Department of Integrated Systems Engineering, The Ohio State University, 1971 Neil Avenue, Columbus, OH 43210-1271, United States of America

Abstract

The charging of battery electric vehicles (BEVs) is a potential source of flexibility and ancillary services to power systems. This paper proposes a two-stage stochastic problem that can be used to optimize the charging of BEVs in a public charging station to provide frequency regulation and energy arbitrage. The model also co-optimizes the use of distributed energy resources, including battery energy storage and photovoltaic solar panels. We demonstrate the performance of the proposed model using a case study based on the Central-Ohio region. The case study shows that proper management of flexibility in BEV charging can provide high-quality frequency regulation services, which is also of significant financial value to the station operator. As such, the modeling methodology that we propose here can further accelerate the adoption of BEVs. This is because the value streams generated by the provision of frequency regulation can reduce the cost of BEV ownership and the net cost of owning and operating a public BEV-charging station.

Keywords: Electric vehicle, vehicle charging, charging control, stochastic optimization, frequency response

1. Introduction

Ancillary services (AS) are necessary to maintain real-time balance between electricity supply and demand. Mismatches between supply and demand can lead to a frequency deviation or other unacceptable power-quality issues. Kempton and Tomić (2005a,b); Dallinger et al. (2011) examine the technical potential and economic value of battery electric vehicles (BEVs) providing some of these types of services.

Providing grid services, including AS, can play an outsize role in enabling greater BEV adoption. A number of works, including formative studies by Kempton and Letendre (1997); Denholm and Letendre (2007), show that the total net cost of BEV ownership can be significantly reduced through the revenues that can be earned by providing grid services. The revenues that are generated from the provision of such services can also incentivize the deployment of public BEV-charging stations. There is a massive literature, including the works of Hodgson (1990); Kuby and Lim (2005); Upchurch et al. (2009); Wang and Lin (2009); Wang and Wang (2010); Upchurch and Kuby (2010); Frade et al. (2011); He et al. (2013); Xi et al. (2013); Shi and Zheng (2014); Cai et al. (2014); He et al. (2015); Shahraki et al. (2015); Li et al. (2016); Dong et al. (2016); Wu and Sioshansi (2017a), studying the optimal deployment of public BEV-charging infrastructure. An important consideration that is neglected by much of this literature is how to finance the development of such infrastructure. Fetene et al. (2016) examine the economics of public workplace charging. They find that it is extremely difficult to structure a workplace-charging contract that is mutually beneficial to the BEV and station owners. The provision of grid services can provide an additional value stream to be shared between the counterparties. This may, in turn, ease such contracting difficulties and the associated challenges in financing the construction of a public charging station.

*Corresponding author

Email addresses: wu.1557@osu.edu (Fei Wu), sioshansi.1@osu.edu (Ramteen Sioshansi)

The provision of grid services by BEVs via a public charging station may also help alleviate transactions-costs issues. Bessa and Matos (2012) survey the role of a BEV aggregator, which essentially acts as an intermediary between individual BEV owners and the wholesale electricity market. They indicate that such an entity can play an important role in efficiently allowing collections of BEVs to participate in wholesale markets. Today's wholesale-market designs do not allow individual BEVs to participate in the markets, because they are too small. The owner of a public BEV-charging station, which acts as a BEV aggregator, can also use other resources, such as battery energy storage (BES) and other distributed energy resources (DERs), to provide grid services. Arsie et al. (2009); Drury et al. (2011) examine the value of energy storage providing grid services within restructured wholesale electricity markets.

Studies that examine the value of BEVs providing grid services suggest that much of the associated value is generated through the provision of AS. This is because providing energy service (*e.g.*, by discharging a BEV's battery) is costly due to the associated cycle-life degradation of the battery. Many AS products (*e.g.*, spinning and non-spinning reserves), conversely, entail rarely having to discharge a BEV battery, because the services are rarely needed in real-time. For instance, Sioshansi and Denholm (2010) find that the vast majority of benefits that accrue to a BEV from providing grid services are due to the provision of spinning and non-spinning reserves.

Frequency regulation is a much higher-quality AS product, compared to spinning and non-spinning reserves. Rebours et al. (2007a,b) provide a comprehensive survey of frequency regulation services. The basic premise is that the generation level of frequency regulation providers is modulated up and down on a second-to-second basis to maintain real-time balance between electricity supply and demand in a power system. Because of this quick response time, frequency regulation is often the highest-priced of all AS.

BEVs have the technical potential to serve as frequency regulation sources, further generating value for BEV and charging-station owners. However, providing frequency regulation can be costly if it entails discharging a BEV battery. Xu et al. (2018) show that considering the degradation of a battery can be important in determining how to offer it in the frequency regulation market. On the other hand, Uddin et al. (2017) suggest that light cycling of a BEV's battery, for instance from providing small amounts of frequency regulation, can improve the battery's health. These works and others suggest that the provision of frequency regulation by discharging a BEV's battery may have mixed effects on battery degradation, which may be highly technology-specific and depend on the overall use of the battery. Thus, the station-control model would have to account for the chemistry of each BEV's battery and have knowledge of the BEV's past and potential future usage profile. A further complication is that it is not clear how BEV manufacturers will treat discharging a BEV's battery from the perspective of battery warranties. Given these complexities in understanding the physical and financial implications of additional battery cycling, this paper focuses on BEVs providing frequency regulation by modulating the rate at which they are recharged to respond to the frequency regulation needs of a power system. Thus, we exclude the potentially costly option of discharging a BEV's battery for providing grid services.

Specifically, we examine the case of a public dc fast BEV-charging station that is used to recharge multiple BEVs. The station may also have access to DERs, including BES and photovoltaic (PV) solar panels, the operation of which can be co-optimized with BEV charging to provide grid services. The charging station is assumed to have a limited window of time within which to recharge BEVs. This window provides some flexibility in scheduling charging loads to provide grid services. The station may also use DERs as added sources of flexibility.

We propose a two-stage stochastic optimization model that can be used for scheduling the use of these various sources of flexibility. The model aims to maximize the value of the services that are provided while meeting technical charging-station requirements. Technical constraints can include a transformer capacity, which limits the amount of power that can be imported to or exported from the charging station, the need to fully recharge each BEV within its charging window, and power and energy capacities of the DERs. The proposed model captures uncertainties, including BEV-arrival times and -charging demands, the frequency regulation signal, and PV output. By capturing the relevant dynamics and sources of uncertainty in the charging system the two-stage stochastic optimization problem that we propose is an advance over existing models that appear in the literature. Moreover, the model that we propose can be used in a rolling-horizon fashion to re-optimize the operation of the system (we conduct this on a one-minute basis), which makes

the model practical for real-world station management.

Our model builds upon works in the existing literature that examine the use of distributed resources and controlled BEV charging for the provision of grid services, including frequency regulation. Pantoš (2012) develops a stochastic optimization model, which focuses on uncertainty in BEV-usage patterns, to determine how individual BEVs should participate in energy and AS markets. The resulting tractability issue is addressed by employing scenario reduction, which gives a problem with a manageable scenario tree. This can be contrasted with our method, which dynamically determines the scenario-tree size to give the proper tradeoff between computational complexity and model fidelity. Janjic et al. (2017) develop a multi-objective optimization model that schedules BEV charging for the provision of frequency regulation while minimizing cost. Their model is solved using a genetic algorithm, which does not provide any guarantees on solution optimality. This can be contrasted with our solution algorithm, which provides valid statistical bounds on the quality of the solution that is obtained from the model. Wu and Sioshansi (2017b); Yan et al. (2018) examine the impacts of distributed PV generators and a BES system in improving the operational performance of a BEV charging station. Wu and Sioshansi (2017b) employ a rolling-horizon stochastic optimization-based approach, on which we base the methodology that we use in this paper. Yan et al. (2018) develop a four-stage hierarchical-optimization framework, which makes planning decisions at day-ahead, hour-ahead, and real-time time frames to minimize the operating cost of the charging station while also maximizing BEV-owners' satisfaction.

There are other works in the extant literature that use different modeling and algorithmic approaches to optimize the operation of BEV-charging stations. Amini et al. (2018) use a decentralized co-ordination scheme that is based on Dantzig-Wolfe decomposition for scheduling BEV charging. The BEV aggregator solves the master problem, which aims to schedule BEV charging for optimal participation in the day-ahead energy market. Individual BEV owners solve subproblems that are co-ordinated by the master problem. The key novelty of their work is that charging co-ordination is handled in a decentralized manner, with minimal information exchange between BEV owners. However, their model is deterministic and does not consider the complexities that our work does. Cao et al. (2018) propose a system to co-ordinate, manage, and schedule BEV charging with the aim of minimizing drivers' wait times while respecting the capacity of the charging station. Their work does not focus on the provision of grid services, such as frequency regulation. Wenzel et al. (2018) develop a modelling framework for a BEV aggregator to provide ancillary services, which *can* be provided by discharging BEV batteries. Their work employs model predictive control, which does not provide the same types of optimality guarantees that our methodology does.

In light of this existing literature, our work makes two primary contributions. First, we employ a two-stage stochastic optimization framework to control the BEV-charging station in a rolling-horizon fashion. The uncertainties that the charging station faces are not truly revealed in a two-stage nature (*i.e.*, in the real-world, these uncertainties are revealed in a fully sequential manner). Nevertheless, we demonstrate that our two-stage optimization model provides high-quality solutions. Second, we adapt a sample-average approximation (SAA) approach to efficiently solve the model. Importantly, we are able to solve the optimization models on standard computing hardware (*i.e.*, without the use of a high-performance computing system) in less than one minute. This means that the proposed model could be used for real-time control of a BEV-charging station.

The remainder of this paper is organized as follows. Section 2 details the proposed two-stage stochastic optimization model while Section 3 outlines the solution algorithm that we employ to efficiently obtain solutions with statistically valid bounds on optimality. Section 4 summarizes data for a numerical case study, which is based on the Central-Ohio region. This case study is used to demonstrate the model and case-study results are presented in Section 5. Section 6 concludes.

2. Model

Our model considers the case of a public BEV-charging station that is connected to the bulk power system through a distribution transformer. This transformer may be used to serve BEV-charging loads as well as other non-BEV-charging loads (*e.g.*, the charging station may be co-located with a retail shopping center, which is served by the same distribution circuit). The charging station may have DERs, including

BES and PV solar panels, installed. In addition to serving BEV-charging and non-BEV-charging loads, the station can also participate in the wholesale market to provide energy or frequency regulation services.

We formulate the charging-station management problem as a two-stage stochastic optimization problem. The first stage represents the current time step, which in our model is taken to be a single minute. We use the notational convention that the current (stage-one) time step is minute j, while all other time steps are denoted minute t. All parameters and decisions at or before minute j are deterministic. The second stage represents the remaining time steps until the end of the optimization horizon. Second-stage parameters can be stochastic and this randomness is characterized through scenarios, ω.

2.1. Model Notation

We begin by defining model notation.

2.1.1. Parameters and Sets

$\bar{H}$	Nameplate capacity of BEV chargers [kW].
$\bar{R}$	Nameplate transformer capacity [kW].
$R^C(\cdot)$	Penalty for operating transformer above nameplate capacity [$/min].
$\bar{S}^{E,+}$	Maximum state of charge (SOC) of BES [kW-min].
$\bar{S}^{E,-}$	Minimum SOC of BES [kW-min].
$\bar{S}^P$	Power capacity of BES [kW].
T	Optimization horizon [min].
W	Charging window for flexible EVs [min].
μ^c	BES charging efficiency.
μ^d	BES discharging efficiency.
ϕ	Price premium for unsatisfied frequency regulation.
Ω	Set of second-stage scenarios.

We assume that some of the BEVs arriving to the charging station are flexible in that their charging demands can be met at any point within a fixed W-minute window of time, so long as they are fully recharged within this window. This charging window is assumed to be sufficiently wide that every flexible BEV can be fully recharged within it. This assumption guarantees problem feasibility. We assume that all flexible BEVs have the same charging window, mainly to ease the model notation. In practice, the flexibility windows of BEVs may vary. It is a simple extension of our model to make the flexibility windows differ for each BEV. The parameter, ϕ, is used to penalize unfulfilled demand for frequency regulation energy that the station has committed to provide. This penalty is applied as a multiplicative factor of the energy price (*cf.* Section 2.2 for details).

2.1.2. Deterministic State Parameters

F_t	Total charging demand of flexible BEVs that arrived to the charging station in minute t [kW-min].
$\bar{f}_t$	Total charging demand of flexible BEVs that arrived to the charging station in minute t that has been satisfied as of the beginning of minute j [kW-min].
L_j	Minute-j inflexible electric load [kW].
N_t	Total number of flexible BEVs that arrived to the charging station in minute t.
p_j	Minute-j electricity price [$/kW-min].
p_j^C	Minute-j frequency regulation-capacity price [$/kW-min].
V_j	Minute-j PV output [kW].
x_j	SOC of BES at beginning of minute j [kW-min].
δ_j^d	Minute-j regulation-down dispatch-to-contract ratio [per unit (p.u.)]
δ_j^u	Minute-j regulation-up dispatch-to-contract ratio [p.u.].

Following the work of Xi et al. (2014), we model the frequency regulation signal using so-called dispatch-to-contract ratios, which we denote δ_j^u and δ_j^d. These ratios indicate the amount of frequency regulation energy that the charging station must provide in real-time in each minute, on a p.u. basis relative to the amount of frequency regulation capacity that the station has committed itself to providing. In reality, a resource that is providing frequency regulation must respond to a control signal that is updated on the

time scale of seconds. Thus, the dispatch-to-contract ratios represent the aggregation of these signals over a minute, as they indicate how much energy in net the charging station must provide to respond to the signal. We also define the state-parameter vector, $\xi_j = (F_t, \bar{f}_t, L_j, N_t, p_j, p_j^C, V_j, x_j, \delta_j^d, \delta_j^u)$.

2.1.3. Stochastic State Parameters

$F_{t,\omega}$ Total charging demand of flexible BEVs that arrive to the charging station in minute t of scenario ω [kW-min].
$L_{t,\omega}$ Minute-t/scenario-ω inflexible energy load [kW].
$N_{t,\omega}$ Total number of flexible BEVs that arrive to the charging station in minute t of scenario ω [kW-min].
$p_{t,\omega}$ Minute-t/scenario-ω electricity price [$/kW-min].
$p^C_{t,\omega}$ Minute-t/scenario-ω frequency regulation-capacity price [$/kW-min].
$V_{t,\omega}$ Minute-t/scenario-ω PV output [kW].
$\delta^u_{t,\omega}$ Minute-t/scenario-ω regulation-up dispatch-to-contract ratio [p.u.].
$\delta^d_{t,\omega}$ Minute-t/scenario-ω regulation-down dispatch-to-contract ratio [p.u.].

Let $\psi_{t,\omega} = (F_{t,\omega}, L_{t,\omega}, N_{t,\omega}, p_{t,\omega}, p^C_{t,\omega}, V_{t,\omega}, \delta^d_{t,\omega}\delta^u_{t,\omega})$ be a vector of minute-t/scenario-ω stochastic state parameters and $\psi_\omega = (\psi_{j+1,\omega}, \ldots, \psi_{j+T,\omega}) \in \Psi$ be a stochastic-parameter vector from minute $j+1$ to the end of the problem horizon. These vectors define the second-stage scenarios.

2.1.4. First-Stage Decision Variables

e^b_j Minute-j power purchases from the power system [kW].
e^c_j Minute-j power charged into BES [kW].
e^d_j Minute-j power discharged from BES [kW].
e^{down}_j Minute-j served regulation-down power [kW].
e^r_j Minute-j frequency regulation-capacity commitment [kW].
e^s_j Minute-j power sales to the power system [kW].
e^{up}_j Minute-j served regulation-up power [kW].
f_j Total minute-j power provided to recharge flexible BEVs [kW].
$f_{j,\tau}$ Total minute-j power provided to recharge flexible BEVs that arrived to the charging station in minute τ [kW].
s^{down}_j Minute-j unserved regulation-down power [kW].
s^{up}_j Minute-j unserved regulation-up power [kW].
v_j Minute-j tranformer overload [kW].
x_{j+1} Beginning minute-$(j+1)$ SOC of the BESS [kW-min].

We define $a_j = (e^b_j, e^c_j, e^d_j, e^{\text{down}}_j, e^r_j, e^s_j, e^{\text{up}}_j, f_j, f_{j,\tau}, s^{\text{down}}_j, s^{\text{up}}_j, v_j, x_{j+1})$ as the vector of first-stage minute-j decision variables.

2.1.5. Second-Stage Decision Variables

$e^b_{t,\omega}$ Minute-t/scenario-ω power purchases from the power system [kW].
$e^c_{t,\omega}$ Minute-t/scenario-ω power charged into BES [kW].
$e^d_{t,\omega}$ Minute-t/scenario-ω power discharged from BES [kW].
$e^{\text{down}}_{t,\omega}$ Minute-t/scenario-ω served regulation-down power [kW].
$e^r_{t,\omega}$ Minute-t/scenario-ω frequency regulation-capacity commitment [kW].
$e^s_{t,\omega}$ Minute-t/scenario-ω power sales to the power system [kW].
$e^{\text{up}}_{t,\omega}$ Minute-t/scenario-ω served regulation-up power [kW].
$f_{t,\omega}$ Total minute-t/scenario-ω power provided to recharge flexible BEVs [kW].
$f_{t,\tau,\omega}$ Total minute-t/scenario-ω power provided to recharge flexible BEVs that arrive to the charging station in minute τ [kW].
$s^{\text{down}}_{t,\omega}$ Minute-t/scenario-ω unserved regulation-down power [kW].
$s^{\text{up}}_{t,\omega}$ Minute-t/scenario-ω unserved regulation-up power [kW].
$v_{t,\omega}$ Minute-t/scenario-ω transformer overload [kW].

$x_{t+1,\omega}$ Beginning minute-$(t+1)$/scenario-ω SOC of the BES [kW-min].

The second-stage decision variables define the operating strategies if scenario ω is realized. Scenario ω is a sample path, which is defined by the stochastic state parameters from minute $j+1$ to $j+T-1$ (*i.e.*, $t \in j+1,\ldots,j+T-1$). We define $u_{t,\omega} = (e^b_{t,\omega}, e^c_{t,\omega}, e^d_{t,\omega}, e^{\text{down}}_{t,\omega}, e^r_{t,\omega}, e^s_{t,\omega}, e^{\text{up}}_{t,\omega}, f_{t,\omega}, f_{t,\tau,\omega}, s^{\text{down}}_{t,\omega}, s^{\text{up}}_{t,\omega}, v_{t,\omega}, x_{t+1,\omega})$ as the minute-t/scenario-ω decision variable-vector and $u_\omega = (u_{j+1,\omega},\ldots,u_{j+T,\omega})$ as the scenario-ω second-stage decision-variable vector.

2.2. Model Formulation

To formulate the station-management problem, we first define $B_j = j-W+1,\ldots,j$ as the set of time steps with the property that BEV arrivals that occurred during B_j are still in their charging window as of minute j. We also define $\Phi_j = j+1,\ldots,j+T$ as the second-stage time steps.

We next define the minute-j station-operation cost as:

$$c_j(a_j,\xi_j) = p_j\cdot(e^b_j - e^s_j) + R^C(v_j) - p^C_j e^r_j + p_j\cdot(1+\phi)(s^{\text{up}}_j + s^{\text{down}}_j),$$

which is the sum of four cost terms. The first is the net cost of purchasing energy from and selling energy to the power system. The second is the cost incurred if the transformer that connects the charging station to the power system is overloaded. This cost, which is assumed to be convex piecewise-linear, represents the degradation of the transformer which accelerates its eventually needing to be replaced. The third term is the revenue earned by the charging station for providing frequency regulation capacity. The fourth term is the penalty incurred for unserved frequency regulation power in real-time. We assume that this penalty is a multiplicative premium above the prevailing energy price.

We analogously define the second-stage scenario-ω cost, as of minute j, as:

$$c_\omega(u_\omega,\psi_\omega) = \sum_{t\in\Phi_j}\left[p_{t,\omega}\cdot(e^b_{t,\omega} - e^s_{t,\omega}) + R^C(v_{t,\omega}) - p^C_{t,\omega}e^r_{t,\omega} + p_{t,\omega}\cdot(1+\phi)(s^{\text{up}}_{t,\omega} + s^{\text{down}}_{t,\omega})\right]. \tag{1}$$

We can then formulate the station-management problem as:

$$\min\ c_j(a_j,\xi_j) + \mathbb{E}\left[c_\omega(u_\omega,\psi_\omega)\right] \tag{2}$$

$$\text{s.t. } e^b_j + e^d_j + e^{\text{down}}_j + V_j = e^s_j + e^c_j + e^{\text{up}}_j + f_j + L_j \tag{3}$$

$$v_j + \bar{R} \geq e^b_j - e^s_j \tag{4}$$

$$-v_j - \bar{R} \leq e^b_j - e^s_j \tag{5}$$

$$x_{j+1} = \hat{x}_j + \mu^c e^c_j - e^d_j/\mu_d \tag{6}$$

$$\bar{S}^{E,-} \leq x_{j+1} \leq \bar{S}^{E,+} \tag{7}$$

$$e^c_j, e^d_j \leq \bar{S}^P \tag{8}$$

$$f_{j,\tau} \leq \bar{H}\cdot N^\tau_j; \quad \forall\tau\in B_j \tag{9}$$

$$f_j = \sum_{\tau\in B_j} f_{j,\tau} \tag{10}$$

$$f_{j,\tau} \leq F_\tau - \bar{f}_\tau; \quad \forall\tau\in B_j \tag{11}$$

$$F_\tau - \bar{f}_\tau - f_{j,\tau} \leq \bar{H}\cdot N_\tau\cdot(W-j+\tau-1); \quad \forall\tau\in B_j \tag{12}$$

$$e^r_j \leq \bar{R} \tag{13}$$

$$e^r_j = e^r_{j-1};\ \text{if } (j \bmod 60)\neq 0 \tag{14}$$

$$e^{\text{down}}_j \leq \delta^d_j e^r_j \tag{15}$$

$$e^{\text{up}}_j \leq \delta^u_j e^r_j \tag{16}$$

$$s^{\text{down}}_j \geq \delta^d_j e^r_j - e^{\text{down}}_j \tag{17}$$

$$s^{\text{up}}_j \geq \delta^u_j e^r_j - e^{\text{up}}_j \tag{18}$$

$$a_j \geq 0 \tag{19}$$

$$e^b_{t,\omega} + e^d_{t,\omega} + e^{\text{down}}_{t,\omega} + V_{t,\omega} = e^s_{t,\omega} + e^c_{t,\omega} + e^{\text{up}}_{t,\omega} + f_{t,\omega} + L_{t,\omega}; \quad \forall t \in \Phi_j; \omega \in \Omega \tag{20}$$

$$v_{t,\omega} + \bar{R} \geq e^b_{t,\omega} - e^s_{t,\omega}; \quad \forall t \in \Phi_j; \omega \in \Omega \tag{21}$$

$$-v_{t,\omega} - \bar{R} \leq e^b_{t,\omega} - e^s_{t,\omega}; \quad \forall t \in \Phi_j; \omega \in \Omega \tag{22}$$

$$x_{j+2,\omega} = x_{j+1} + \mu^c e^c_{j+1,\omega} - e^d_{j+1,\omega}/\mu_d \tag{23}$$

$$x_{t+1,\omega} = x_{t,\omega} + \mu^c e^c_{t,\omega} - e^d_{t,\omega}/\mu_d; \quad \forall t \in \Phi_j; \omega \in \Omega \tag{24}$$

$$\bar{S}^{E,-} \leq x_{t,\omega} \leq \bar{S}^{E,+}; \quad \forall t \in \Phi_j \backslash j+1; \omega \in \Omega \tag{25}$$

$$e^c_{t,\omega}, e^d_{t,\omega} \leq \bar{S}^P; \quad \forall t \in \Phi_j; \omega \in \Omega \tag{26}$$

$$f_{t,\tau,\omega} \leq \bar{H} \cdot N^\tau_{t,\omega}; \quad \forall t \in \Phi_j; \tau \in B_t; \omega \in \Omega \tag{27}$$

$$f_{t,\omega} = \sum_{\tau \in B_t} f_{t,\tau,\omega}; \quad \forall t \in \Phi_j; \omega \in \Omega \tag{28}$$

$$\sum_{t=j+1}^{\tau+W} f_{t,\tau,\omega} + f_{j,\tau} = F_\tau - \bar{f}_\tau; \quad \forall \tau \in B_j; \omega \in \Omega \tag{29}$$

$$\sum_{t=\tau}^{\tau+W} f_{t,\tau,\omega} = F_\tau; \quad \forall \tau = j+1, \ldots, j+T-W; \omega \in \Omega \tag{30}$$

$$\sum_{t=\tau}^{j+T} f_{t,\tau,\omega} \leq F_\tau; \quad \forall \tau \in B_{j+T}; \omega \in \Omega \tag{31}$$

$$F_\tau - \sum_{t=\tau}^{j+T} f_{t,\tau,\omega} \leq \bar{H} \cdot N_{\tau,\omega} \cdot (W - j - T + \tau); \quad \forall \tau \in B_{j+T}; \omega \in \Omega \tag{32}$$

$$e^r_{t,\omega} \leq \bar{R}; \quad \forall t \in \Phi_j; \omega \in \Omega \tag{33}$$

$$e^r_{t,\omega} = e^r_{t-1,\omega}; \quad \forall t \in \Phi_j : (t \bmod 60) \neq 0; \omega \in \Omega \tag{34}$$

$$e^{\text{down}}_{t,\omega} \leq \delta^d_{t,\omega} e^r_{t,\omega}; \quad \forall t \in \Phi_j; \omega \in \Omega \tag{35}$$

$$e^{\text{up}}_{t,\omega} \leq \delta^u_{t,\omega} e^r_{t,\omega}; \quad \forall t \in \Phi_j; \omega \in \Omega \tag{36}$$

$$s^{\text{down}}_{t,\omega} \geq \delta^d_{t,\omega} e^r_{t,\omega} - e^{\text{down}}_{t,\omega}; \quad \forall t \in \Phi_j; \omega \in \Omega \tag{37}$$

$$s^{\text{up}}_{t,\omega} \geq \delta^u_{t,\omega} e^r_{t,\omega} - e^{\text{up}}_{t,\omega}; \quad \forall t \in \Phi_j; \omega \in \Omega \tag{38}$$

$$u_\omega \geq 0; \quad \forall \omega \in \Omega \tag{39}$$

Objective function (2) minimizes the expected cost of operating the charging station over the T-minute optimization horizon. The model has two sets of constraints—constraints (3)–(19) pertain to the first stage while constraints (20)–(39) pertain to the second stage.

Constraint (3) imposes load balance on the charging station. Constraints (4) and (5) define the amount that the transformer is overloaded in terms of the net power that is exchanged between the charging station and the power system. Constraints (6)–(8) pertain to the BES. The first defines how the SOC of the BES evolves from minute j to $(j+1)$, the second imposes the bounds on the minute-$(j+1)$ SOC, and the third imposes the power capacity on charging and discharging.

Constraints (9)–(12) pertain to BEV charging. Constraints (9) restrict the total amount of charging to BEVs that arrive in minute τ based on the chargers' assumed capacities and the number of BEV arrivals. Constraint (10) defines f_j as the sum of the $f_{j,\tau}$'s. Constraints (11) restrict the amount of energy charged into BEVs that arrived in minute τ to be no greater than the remaining unfulfilled charging demand. Constraints (12) ensure that any remaining unfulfilled BEV-charging demands at the end of minute j can be feasibly met if the BEVs are charged at the chargers' power capacity for the remainder of the charging window. We model BEV charging assuming a linear relationship between energy that is recharged and the

SOC of a BEV's battery. In some cases a nonlinear or piecewise-linear relationship may be more appropriate. For instance, BEV manufacturers may reduce the maximum charging rate as the SOC of a BEV's battery approaches the maximum.

Constraints (13)–(18) relate to offering and serving frequency regulation commitments. Constraint (13) restricts the amount of frequency regulation capacity that the charging station can provide to be less than the transformer capacity. Constraint (14) imposes the restriction that the charging station can only change its frequency regulation commitment on an hourly basis, which is a typical rule in most wholesale markets. This constraint also enforces a time dynamic in the provision of frequency regulation. The charging station must commit itself *a priori* to the amount of frequency regulation capacity that it will provide, before knowing how much energy it must provide (which is governed by the dispatch-to-contract ratios, which are random in subsequent time steps). Constraints (15) and (16) bound the amount of frequency regulation power provided in real-time to be less than the amount requested by the system, which is defined as the product of the dispatch-to-contract ratio and the frequency regulation commitment. Constraints (17) and (18) define the unserved frequency regulation power in terms of the served power. Finally, constraint (19) imposes non-negativity on all of the first-stage decision variables.

The second-stage constraints largely have the same interpretation as the first-stage constraints, with the notable difference that they are imposed on a per-minute and -scenario basis. Constraints (20) impose load-balance on the charging station. Constraints (21) and (22) define transformer loading.

Constraints (23) and (24) define the evolution of the BES SOC, constraints (25) impose bounds on the BES SOC, and constraints (26) impose power limits on BES charging and discharging. Our model does not include constraints that restrict the ending SOC of the BES to equal its starting SOC. Such constraints can be used to ensure that an energy storage system is not fully discharged at the end of the planning horizon. In a sense, constraints of this type heuristically ascribe carryover value to energy that remains in storage at the end of the planning horizon. We, instead, employ the technique that is adopted by Sioshansi et al. (2009) to assign carryover value to stored energy. This is done by including additional operating periods in the optimization model that goes beyond the planning horizon. Including these additional operating periods ensures that operating decisions over the planning horizon take account of future operation of the energy storage system (after the planning horizon). Our two-stage model structure accomplishes the same because only decisions that are made for the first stage (*i.e.*, the first minute) are binding (in the sense that they are implemented). Operating decisions for minutes $j+1,\ldots,j+T$ are not binding and are instead included in the model so that current-minute decisions account for future charging-station operations.

Constraints (27)–(32) pertain to BEV recharging. Constraints (27) restrict the total amount of recharging energy that is provided based on the number of BEVs and the power capacity of the charging stations. Constraints (28) define the $f_{t,\omega}$'s in terms of the $f_{t,\tau,\omega}$'s. Constraints (29) ensure that all BEVs that have already arrived as of minute j are fully recharged within the charging window. Constraints (30) ensure that all flexible BEVs that arrive after minute j and that have a charging window that ends before the T-minute optimization horizon are fully recharged. Constraints (31) ensures that the remaining flexible BEVs are not overcharged while constraints (32) ensure that they are charged sufficiently to be able to be fully recharged before their charging windows expire.

Constraints (33)–(38) relate to the provision of frequency regulation in the second stage. Constraints (33) restrict the amount of frequency regulation capacity that the station can provide while constraints (34) only allow the capacity commitment to be changed on an hourly basis. Constraints (35) and (36) bound the amount of frequency regulation power provided to be no greater than the amount requested by the system. Constraints (37) and (38) define the unserved frequency regulation power in terms of the served power. Finally, constraints (39) impose non-negativity on the second-stage decision variables.

3. Solution Method

We use an SAA approach, which is outlined by Bayraksan and Morton (2006, 2011); Shapiro et al. (2014); Wu and Sioshansi (2017b), to solve the proposed station-control problem. This is because the second stage is defined on a sample space, Ψ, which has an uncountably infinite support. SAA allows us to approximate the

second stage by randomly drawing a subset of sample paths, Ψ^l. The resulting SAA problem approximates the true station-control problem. We provide an outline of the SAA approach, which is taken from the work of Wu and Sioshansi (2017b). Interested readers are referred to their work for complete details of the SAA method and its convergence properties.

To give the SAA problem, we first define the feasible region of the first-stage constraints as:

$$A_j = \{a_j | (3) - (19)\},$$

and the feasible region of the second-stage constraints under scenario-ω as:

$$U(\psi_\omega) = \{u_\omega | (20) - (39)\}.$$

We then define $\psi_1, \ldots, \psi_{m_\kappa}$ as m_κ independent and identically distributed (i.i.d.) samples of the second-stage sample paths (*i.e.*, samples of ψ_ω). The κ subscript on m_κ denotes the iteration number of the algorithm that is employed to solve the station-control model (*cf.* Algorithm 1). $\psi_1, \ldots, \psi_{m_\kappa}$ are randomly generated by Monte Carlo simulation. Wu and Sioshansi (2017b) discuss the method used to generate the sequence, $\{m_\kappa\}$, which is integral. The SAA problem is then formulated as:

$$\min_{a_j \in A_j} \left\{ \frac{1}{m_\kappa} \sum_{m=1}^{m_\kappa} \left[c_j(a_j, \xi_j) + \min_{u_m \in U(\psi_m)} c_m(u_m, \psi_m) \right] \right\}, \tag{40}$$

where $c_m(u_m, \psi_m)$ is defined by (1).

Algorithm 1 provides a high-level overview of the SAA method that we employ. Step 1 begins by choosing sample-size sequences, $\{m_\kappa\}$ and $\{l_\kappa\}$, and a termination criterion, Υ. The first sample-size sequence, $\{m_\kappa\}$, is used to generate random samples and resulting SAA problems in each iteration of the algorithm. The second sample-size sequence, $\{l_\kappa\}$, is used in each iteration to estimate the optimality gap of the solution to the SAA problem. In essence, this optimality-gap estimate determines the robustness of the solution that is obtained from the SAA problem to the set of sample paths that is used. This is because the solution that is obtained in iteration κ comes from solving an SAA problem with the sample paths, $\psi_1, \ldots, \psi_{m_\kappa}$. The optimality-gap estimator is then obtained by using this solution with the sample paths, $\psi_1, \ldots, \psi_{l_\kappa}$. The sample-path sequences should both be integral and grow faster than $\mathcal{O}(\log \kappa)$. The termination criterion, Υ, is typically based on the absolute or relative optimality gap.

Algorithm 1 SAA Method

1: **input:** sample-size sequence $\{m_\kappa\}$, $\{l_\kappa\}$, stopping criterion Υ
2: $\kappa \leftarrow 0$
3: **repeat**
4: generate m_κ i.i.d. random samples, $\psi_1, \ldots, \psi_{m_\kappa}$, of second-stage scenarios
5: solve SAA problem (40) using L-shaped method
6: generate l_κ i.i.d. random samples and optimality-gap estimator
7: $\kappa \leftarrow \kappa + 1$
8: **until** Υ is satisfied

Steps 3–8 are the main iterative loop. In Step 4 of iteration κ, the m_κ i.i.d. random samples are generated to define an SAA problem. This problem is solved using an L-shaped method (*i.e.*, Benders's decomposition) in Step 5. In Step 6, we use the averaged two-replication procedure that is proposed by Bayraksan and Morton (2006) to compute an optimality-gap estimator and its variance. More specifically, l_κ i.i.d. samples of the random variables are generated to estimate the optimality gap of the solution to the SAA problem that is found in Step 5. This gap estimator is used in the termination criterion, Υ. The iterative process repeats, with the sample sizes increasing, until stopping criterion Υ, is satisfied.

4. Case-Study Data

The proposed station-control model is demonstrated using a case study that is based on a simulated public BEV-charging station with multiple dc fast chargers that is co-located with a commercial shopping center in northeastern Columbus, Ohio. As such, the charging station is in the service territory of AEP Ohio, which is the distribution utility in Central Ohio. Moreover, the charging station is assumed to participate in the PJM Interconnection market, as the AEP service territory is in PJM's footprint. We do not explicitly specify the number of chargers that are installed at the station. Rather, we assume that there is a sufficient number of chargers installed to ensure that there is a free charger available with which an arriving BEV can commence charging immediately. This section describes the case study's assumptions and input data.

4.1. Temporal Resolution and Case-Study Simulation

In keeping with the model formulation that is presented in Section 2, the case study assumes a one-minute temporal resolution. Station operations are simulated over a representative year, using data for the year 2013.

The model is used in a rolling-horizon fashion, whereby the two-stage stochastic problem is re-optimized one minute at a time with updated deterministic and stochastic state parameters. The deterministic state parameters, which represent actual system states (*e.g.*, actual PV production or number of flexible BEVs arriving in minute j), are simulated using distributions that are fitted to data or via Monte Carlo simulation (*cf.* Sections 4.2–4.7 for descriptions of how the different random state parameters are simulated). The stochastic state parameters, which are sample paths representing forecasts of future system conditions, are generated in the same way.

Thus, our rolling-horizon technique allows sample paths of future stochastic state parameters to be updated on a minute-to-minute basis. In practice, sample paths of many of these parameters may not be updated that frequently. For instance, energy and frequency regulation prices are updated at five-minute or longer time intervals by PJM. We update these parameters at the same temporal resolution. The model uses a $T = 90$-minute optimization horizon, which is sufficiently long to account for the charging windows of flexible BEVs and the hour-long persistence of frequency regulation commitments.

4.2. Battery Electric Vehicle Characteristics

BEV-travel patterns are modeled by bootstrapping from tour-record data that are obtained from the Mid-Ohio Regional Planning Commission. The tour-record data, details of which are given by Sener et al. (2009), contain modeled typical daily driving profiles for the 1.1 million light-duty vehicles in the Central-Ohio region. We assume that BEVs constitute 8% of this light-duty vehicle fleet and simulate BEV-related state parameters by randomly selecting 8% of the vehicles in the tour-record data to be BEVs.

Once we randomly select the subset of vehicles that are BEVs, we use a shortest-time-path model to determine the exact driving path that each simulated BEV takes. We next determine the SOC of each BEV's battery as it travels along its path. We do this by assuming that each BEV has a battery capacity of 24 kWh and a driving efficiency of 0.1875 kWh/km. This driving efficiency takes account of the average energy that is used to propel the BEV and the efficiency losses that are incurred when recharging the BEV's battery. We then assume that any BEV that comes within a 1.6-km (1.0-mile) radius of the charging station and that has a battery SOC below 50% at that time stops at the station to recharge.

We assume that 80% of BEVs are flexible, in that their charging can be scheduled by the station within a $W = 40$-minute window. The remaining BEVs are assumed to be inflexible and their charging demands are added to the non-BEV loads in determining L_j and $L_{t,\omega}$.

4.3. Transformer Characteristics

The charging station is connected to the power system through an $\bar{R} = 500$-kVA transformer, which is shared with the buildings in the commercial retail center where the station is located. A transformer can be operated above its design capacity. Doing so can reduce its usable life below the standard 20-year design life, however.

We estimate the effect of this accelerated aging using a thermal model, which is based on the work of Gong et al. (2011), that simulates the effects of transformer loading on the temperature of its windings. More specifically, we use the model to simulate the impacts of different load profiles on reducing the transformer's life. This reduction in service life is combined with an assumed $10000 transformer-replacement cost, to derive a convex piecewise-linear penalty function for operating the transformer above its capacity.

Our assumed parameters result in the transformer-overload-penalty function:

$$R^c(v_t) = \begin{cases} 1.16v_t & \text{if } v_t \in [0, 200), \\ 42.65(v_t - 0.4\bar{R}) + 232.70 & \text{if } v_t \in [200, 300), \\ 764.62(v_t - 0.6\bar{R}) + 4497.35 & \text{if } v_t \in [300, 400), \\ 12309.73(v_t - 0.8\bar{R}) + 80959.50 & \text{if } v_t \in [400, +\infty), \end{cases}$$

which behaves in the way expected. The assumed 500-kVA transformer can be operated at up to 700 kVA (*i.e.*, 40% above its design capacity) with relatively modest degradation in its service life that translates into a cost of $1.16/kVA. As the transformer is more highly loaded, the service life that is lost increases drastically with significantly higher associated costs.

4.4. Non-Electric Vehicle Load

We model the non-BEV loads using data from the year 2013 that are provided by AEP Ohio. The data consist of anonymized load profiles for numerous 500-kVA commercial transformers, recorded at a 15-minute time resolution. These types of commercial transformers tend to have fairly persistent demand patterns from day to day. This is because commercial building load is largely driven by space conditioning needs (which tend to be similar on a seasonal basis) and the behavior of building occupants. As such, we fit an ARIMA $(2, 1, 0) \times (0, 1, 1)_{96}$ model to generate sample paths of non-BEV loads (in addition to the loads of inflexible BEVs, as discussed in Section 4.2).

4.5. Solar Photovoltaic Generation

The charging station is assumed to have a 200-kW PV system installed. However, there are no solar PV panels at the assumed location of the charging station. Thus, we do not have access to actual PV-production data. We use modeled historical weather data from the year 2013, which are obtained from the National Solar Radiation Database, and the PVWatts software package to model actual PV production at the station location at a one-minute time resolution. Sengupta et al. (2014b,a) describe the National Solar Radiation Database while Dobos (2014) details the PVWatts model.

PV production at a one-minute time resolution can be extremely noisy and difficult to forecast, due to short-lived transient effects (*e.g.*, a brief cloud formation). Hourly-averaged PV production, on the other hand, can smooth-out this noise. We also find that the residuals between hourly-averaged and one-minute PV production follow a mean-zero Laplace distribution. Thus, for purposes of PV simulation, we first fit an ARIMA $(5, 2, 0) \times (2, 1, 0)_{24}$ model to hourly-averaged PV production data. This ARIMA model is used to simulate and forecast hourly-average PV production in our case study. We then use a fitted Laplace distribution to simulate residuals between hourly-average and one-minute PV production, to generate sample paths of one-minute PV production.

4.6. Energy and Frequency Regulation-Capacity Prices

We model energy and frequency regulation-capacity prices using historical data for the AEP Zone in the PJM Interconnection market for the year 2013. Energy prices relate to the cost of operating the charging station as well as any revenues that are earned from selling excess PV or BES energy. The energy prices average $44.03/MWh, have a standard deviation of $57.44/MWh, and range between -$55.20/MWh and $1851.29/MWh over the year that is modeled. Using these historical data, we fit 24 log-normal distributions to the prices corresponding to each hour of the day. Frequency regulation prices relate to revenues that are earned for providing frequency regulation service. These prices average $43.70/MW-h, have a standard deviation of $104.07/MW-h, and range between $0.01/MW-h and $3303.87/MW-h over the year that is modeled. The same approach (*i.e.*, using 24 log-normal distributions corresponding to each hour of the day) is also used to model frequency regulation-capacity prices.

4.7. Frequency Regulation-Dispatch-to-Contract Ratios

We model the dispatch-to-contract ratios using historical frequency regulation-signal data that are obtained from PJM Interconnection for the year 2013. We fit 24 Gaussian distributions to the historical frequency regulation-signal data for each hour of the day. The dispatch-to-contract ratios in our case study are simulated using these Gaussian distributions, which are truncated to ensure that the ratios are bounded between 0 and 1 (dispatch-to-contract ratios outside of this range are physically meaningless).

4.8. Battery Energy Storage Characteristics

We assume that the BES has upper and lower bounds on its SOC of $\bar{S}^{E,+} = 8400$ kW-min (140 kWh) and $\bar{S}^{E,-} = 2400$ kW-min (40 kWh) and a power capacity of $\bar{S}^{P} = 200$ kW, respectively. We also assume charging and discharging efficiencies of $\mu^{c} = \mu^{d} = 0.99$. These values are typical for lithium-ion BES, as reported by Xi and Sioshansi (2016b). We neglect the degradation effects of cycling the BES in our case study. Degradation effects can be captured by adding a term to the objective function that accounts for the implicit opportunity cost, or by successively updating the available energy storage capacity of the BES from one operating period to the next. Xi and Sioshansi (2016a) study the impacts of degradation in using distributed BES for the provision of grid services. While they find some impacts, they are overall relatively muted. Degradation of the BES should also be contrasted with that of BEVs' batteries (which is why we do not consider discharging BEVs' batteries to provide frequency regulation). The primary purpose of a BEV's battery is for transportation. As such, energy storage capacity is critically important for a BEV to be a viable transportation technology. The energy storage capability of a stationary BEV system does not entail the same level of criticality.

4.9. Sensitivity Analyses

The performance of the charging station and the operational strategies that are found by the model are affected by a number of factors. We explore these effects through six sensitivity analyses, which are summarized in Table 1. The table shows the cases that we examine, which differ in whether BES is installed, the bias in the frequency regulation signal, the power capacity of the BEV chargers, $\bar{H}$, and the size of the BEV. Case 1 is the base case, while Cases 2–6 are sensitivity cases in which a single factor is changed. Contrasting model results between each of these cases and Case 1 allows us to understand the impact of each factor.

Table 1: Sensitivity Cases Examined

Case	$\bar{H}$	BES	Frequency Regulation Bias [%]	BEV Size
1 (Base)	100	Installed	0%	Standard
2 (No BES)	100	Not Installed	0%	Standard
3 (Regulation-Down Bias)	100	Installed	−5%	Standard
4 (Regulation-Up Bias)	100	Installed	+5%	Standard
5 (Large Charger)	200	Installed	0%	Standard
6 (Large BEV)	100	Installed	0%	Standard

We study the bias in the frequency regulation signal by modeling the frequency regulation signal in a two-step process. First, in each minute we randomly generate a Bernoulli trial to determine if there is an 'up' or 'down' frequency regulation signal in that particular minute. Once the direction of the signal is known, the dispatch-to-contract ratio is randomly simulated using the Gaussian distribution of the corresponding hour. In Cases 1, 2, 5, and 6 the Bernoulli trials are unbiased whereas in the other two cases the Bernoulli trials are biased in one direction or another.

Cases 1–4 and 6 assume 100-kW chargers whereas Case 5 assumes a 200-kW charger. Thus, we implicitly assume that the BEVs and chargers conform to the proposed SAE J1772 standards for dc fast charging. Cases 1–5 assume the standard BEV size, which is given in Section 4.2. Case 6 assumes large BEVs, which

have 50-kWh batteries and 2.1 times the energy consumption of the standard BEVs, but the same 1.6-km/50%-SOC threshold for using the charging station as with the standard BEVs. The purpose of this sensitivity case is to examine the impact of having the charging station more constrained, *vis-à-vis* the transformer capacity and charging window, on its ability to provide frequency regulation.

Although we study a number of sensitivity cases, there are additional cases that could be examined. We limit the sensitivity cases that we analyze for two reasons. One is that despite the fact that Algorithm 1 can solve a single instance of the station-control problem quickly, simulating a full year is time-consuming, as it requires solving 525600 instances of the problem in sequence (*i.e.*, one problem instance for each minute of the year). The second reason is that many possible sensitivity cases would have limited impact on the ability of the charging station to provide frequency regulation, which is the focus of our work. Instead, those cases would mainly affect other aspects of operating the charging station. For instance, Wu and Sioshansi (2017b) examine the impacts of having access to a PV system in a charging station. This previous work finds that a PV system reduces the net load and operating cost of the charging station, by 12% and 58%, respectively, on average. However, a PV system would have limited benefits in increasing the flexibility of the charging station to provide frequency regulation.

5. Case-Study Results

We summarize our case-study results here. Section 5.1 first discusses the results of our base case (Case 1) while Section 5.2 summarizes the results of our sensitivity analyses (Cases 2–6).

5.1. Base-Case Results

Figure 1 summarizes the operation of the charging station between 14:00 and 21:59 on 5 May. The top pane of the figure shows the cumulative charging demand of flexible BEVs and the amount of frequency regulation capacity that is committed and unserved by the charging station. The cumulative BEV-charging demand reflects charging demand that is unmet. The 33 times that the cumulative BEV-charging demand increases correspond to the 33 arrivals of flexible BEVs during the eight-hour period that is shown. Decreases in the charging demand correspond to the flexible BEVs being progressively recharged. The bottom pane of the figure shows energy and frequency regulation prices.

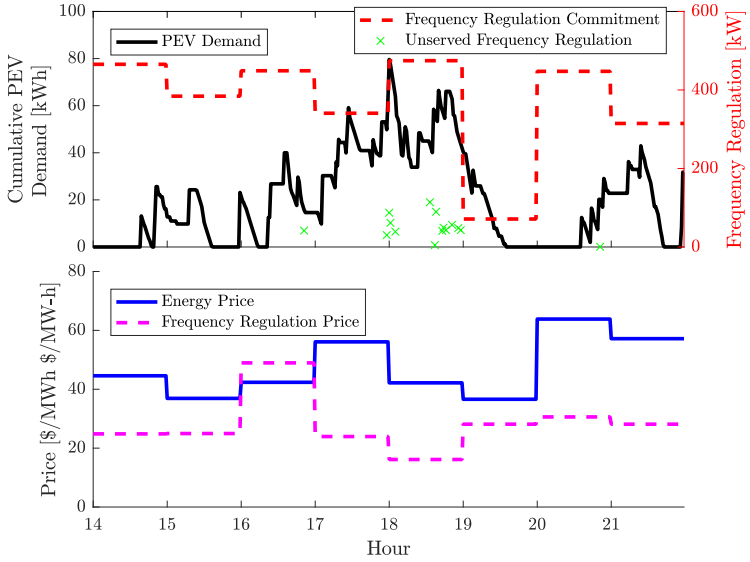

Figure 1: Operation of the Charging Station on 5 May

The provision of frequency regulation capacity is driven by its price, the energy price (which determines the penalty for unserved frequency regulation), and the amount of flexibility (which is largely in the form of

BEV-charging loads), that is available. All eight of the hours that are shown in Figure 1 have relatively high frequency regulation prices of at least \$16/MW-h. As such, the model aims to provide as much frequency regulation as the second-stage scenarios suggest can be feasibly provided. Hour 19 has the fourth-highest frequency regulation price during the eight-hour period that is shown. Nonetheless, the charging station sells less frequency regulation capacity in hour 19 than it does during the other hours. This is due to the relatively few flexible-BEV arrivals that are anticipated in that hour. Indeed, only one flexible BEV arrives during the simulated hour and the charging station has no flexible BEV-charging loads for a 61-minute period of time beginning at 19:35. During this time span, the BES and curtailed output from the PV panels are the only sources of flexibility that the charging station has available. Because more flexible-BEV arrivals are anticipated in hour 20 (four flexible BEVs arrive during the simulated hour), the model sells more frequency regulation capacity in hour 20. The same is true of hour 18, which has the lowest frequency regulation price during the eight hours that are shown. Because significantly more flexible-BEV arrivals are anticipated (seven flexible BEVs arrive during the simulated hour), the charging station has more inherent flexibility with which to serve frequency regulation demands. As such, the model sells more frequency regulation service during hour 18.

Figure 1 also shows that the charging station is not able to fully meet all of its frequency regulation obligations. The station has a frequency regulation shortfall in 15 of 480 minutes that are shown in Figure 1. Hour 18, which has many flexible-BEV arrivals, presents the greatest difficulty in meeting frequency regulation obligations. This is largely due to the charging needs of inflexible BEVs. This finding shows that BEV arrivals represent a 'double-sided sword'—more BEV arrivals typically translate into greater flexibility in the form of flexible BEVs but can also reduce flexibility due to the charging demands of inflexible BEVs. These frequency regulation shortfalls affect the charging station in two ways. In the short-run, the charging station is penalized for frequency regulation shortfalls. This is captured in the objective function of the station-control model. In the long-run, PJM may disqualify a resource from providing frequency regulation if its performance score, which is related to its ability to follow the frequency regulation signal, is too low.

The charging station provides an average (over the year that is simulated) of 6.31 MW-h of frequency regulation capacity daily. This translates into an average daily revenue of \$441.88 from the provision of frequency regulation services (taking into account the penalties that are associated with unfulfilled obligations) and an average net selling price of \$70.01/MW-h. This average selling price of frequency regulation is greater than the annual average price of \$43.70/MW-h (*cf.* Section 4.6). This finding indicates that the model is 'selective' in only providing frequency regulation during high-value hours. This is because the model must ultimately tradeoff the requirement that all BEVs be recharged with the cost of incurring penalties for overloading the transformer. Providing frequency regulation at any time step increases the likelihood that BEV charging must deferred to subsequent time steps. This is to reduce the charging rate and provide frequency response in the current time step. This deferral of BEV charging exacerbates the likelihood of transformer overloads in subsequent time steps.

Over the course of the year the station is able to fully meet its frequency regulation obligation 99.58% of the time. Moreover, during the time periods that the station does not fully meet its frequency regulation obligation, it is able to provide 85.61% of its obligation. These results indicate that our proposed optimization model is able to provide relatively high-quality response to the frequency regulation signal. This is done by properly managing the SOC of the BES, the inherent flexibility in BEV charging, and the amount of frequency regulation capacity sold to the market. The charging station has more difficulty in fulfilling regulation-up as opposed to regulation-down obligations. On average, the station is unable to meet 57 kWh of daily regulation-up calls as opposed to only 6 kWh of regulation-down.

The 500-kW transformer that connects the co-located charging station and commercial building to the power system may have a positive or negative net load. A negative net load implies that the charging station is a net supplier of energy to the power system. This may happen if the station is selling excess PV production or discharging BES. The transformer has a negative net load in about 1400 of the 8760 hours in the year that is examined. We also find that the transformer operates near its 500-kW capacity in about 4000 hours of the year. The transformer is overloaded for two hours over the course of the simulated year, operating at an average of 520 kW during these hours.

5.2. Sensitivity Analyses

Table 2 provides summary statistics, across the days of the simulated year, of daily charging-station operating cost and the net (of penalties for unserved power) revenue that is earned by the charging station for providing frequency regulation. Contrasting these costs and revenues between the six cases provides insights into how the different factors impact the economic performance of the charging station.

Contrasting Cases 1 and 2 shows that BES impacts the charging station in two important ways. First, BES is able to reduce the operating cost of the charging station by providing more flexibility in accommodating BEV-charging loads. This effect is exemplified by the much higher standard deviation of the station-operation cost in Case 2. The greater standard deviation is due to high transformer loading on days when there is insufficient flexibility in BEV charging to keep transformer loading below 500 kW. BES provides added flexibility to accommodate these loads in Case 1. The table also shows that BES allows the charging station to provide more high-value frequency regulation. The station is still able to provide some frequency regulation in Case 2, which primarily comes from the flexibility in managing BEV-charging loads.

Table 2: Mean and Standard Deviation Across the Days of the Simulated Year of Daily Station-Operation Cost and Net Frequency Regulation Revenue in Sensitivity Cases

Case	Operation Cost [$]		Frequency Regulation Revenue [$]	
	Mean	Standard Deviation	Mean	Standard Deviation
1 (Base)	890	1211	442	694
2 (No BES)	2768	5925	225	371
3 (Regulation-Down Bias)	830	1032	450	738
4 (Regulation-Up Bias)	933	1310	429	664
5 (Large Charger)	2466	8110	439	696
6 (Large BEV)	35617	1559	423	290

Cases 3 and 4 show that having a biased frequency regulation signal has a relatively small impact on the economic performance of the charging station. However, we do find that having a negative bias in the signal (*i.e.*, favoring regulation-down) does slightly improve the performance of the charging station relative to an unbiased signal. This is consistent with our findings in the base case that the charging station tends to have more difficulty in serving regulation-up as opposed to -down. This is because the charging station is ultimately a net consumer of energy. A regulation-down signal is met by increasing the charging-station load, which is typically easier to accommodate. One way to address this difference in the charging station's ability to provide regulation-up and -down services is to bifurcate the two products, as is done in the California Independent System Operator market.

Case 5 shows the impact of increasing the power capacity of the BEV chargers. In the other cases, a BEV can be fully recharged in about 14 minutes. This charging time is reduced to seven minutes in Case 5. Comparing the operating cost in Case 5 to Case 1 shows that the increased chargers' capacities has the same impact as removing BES in increasing transformer overloads. This is especially true with inflexible BEVs, which are assumed to begin charging immediately upon arrival at the charging station. The peak load on the transformer increases 13% from about 800 kW in Case 1 to 958 kW in Case 5. Table 2 shows that increasing the chargers' capacities does not have any major impact on frequency regulation revenues.

Case 6 shows that the performance of the charging station is severely impacted by increasing BEV charging demands, which is the net impact of having larger BEVs. The operating cost of the charging station increases by a factor of 40 relative to Case 1. This is largely due to the higher BEV loads resulting in the transformer being overloaded an average of 17 minutes daily in Case 6 as opposed to an average of 0.3 minutes daily in Case 1. Even if transformer-degradation costs are excluded, the daily average cost of operating the charging station is $3067. This is due to the higher BEV charging demands that must be served, but also because the station has significantly less flexibility in scheduling BEV charging. Whereas a BEV can be fully recharged in 14 minutes in Case 1, this charging time increases to 29 minutes in Case 6.

Table 3 summarizes the performance of the charging station in providing frequency regulation services in the sensitivity cases. It shows the average daily provision of frequency regulation capacity to the market, along with the average daily duration and MW-h shortfall in following the regulation-down and -up signals. The table shows that the availability of BES and the size of the BEV-charging loads are the biggest factors in determining how much frequency regulation capacity the charging station provides. As expected, having a negatively biased frequency regulation signal allows the charging station to slightly increase its provision of the service. In all of the cases, except for Case 6, the frequency regulation signal is fully satisfied at least 97% of the time and the station is able to fulfill at least 99% of the regulation power that is requested by the system. This, again, illustrates that our proposed model is able to effectively manage the provision of frequency regulation, regardless of the configuration of the station.

Table 3: Average Daily Frequency Regulation Service Provided in Sensitivity Cases

Case	Frequency Regulation Capacity Provided [MW-h]	Unfulfilled Time [min]		Unfulfilled Power [MW-h]	
		Down	Up	Down	Up
1 (Base)	6.31	0.74	41.99	0.005	0.057
2 (No BES)	3.18	0.70	61.95	0.004	0.078
3 (Frequency-Down Bias)	6.47	0.73	40.63	0.005	0.053
4 (Frequency-Up Bias)	6.07	0.66	41.91	0.005	0.065
5 (Large Charger)	6.30	0.75	38.61	0.005	0.057
6 (Large BEV)	11.49	0.75	148.31	0.005	0.478

Case 6 results in greater difficulty in supplying regulation-up services compared to the other cases. This is due to the high BEV-charging loads relative to the transformer capacity in Case 6. In Cases 1–5 regulation-up service is provided by decreasing BEV-charging loads and deferring BEV recharging until later in the charging window. However, the charging station is limited in following such a strategy in Case 6. This is because the relatively high BEV-charging demands result in a very limited amount of time within which to defer BEV charging. A BEV with an empty battery requires 29 minutes to fully recharge in Case 6. This means that there is only 11 minutes (out of the 40-minute window of recharging time) within which to shift the charging loads of such a BEV. As such, the station-control model must choose between following the regulation-up signal or leaving regulation-up service unserved. The former option may be infeasible (if there is insufficient time remaining in the 40-minute window) or costly (if it entails overloading the transformer in subsequent time step(s) to fully recharge all BEVs). The latter option is also costly, as it entails financial penalities.

Contrasting the performance of the charging station in Case 6 can also provide a basis on which to infer the impacts of changing the charging window or transformer characteristics. Increasing the charging window or any changes that lower the cost of transformer loading (*e.g.*, greater transformer capacity, slower degradation, or lower replacement cost) should improve the performance of the charging station in supplying frequency regulation in Case 6. These types of changes likely have more muted effects in the other cases, where the provision of frequency regulation is not as constrained as in Case 6.

Our proposed optimization model and solution technique are implemented using CPLEX version 12.6.1. When run on a computer with a 3.0 GHz Intel Pentium G3220 Processor and 16 GB of memory, each instance of the one-minute station-control models requires an average of about 600 second-stage scenarios and 40 seconds of CPU time to run and achieve the desired solution quality. Thus, the model can be tractably solved in the rolling-horizon fashion that we propose.

6. Conclusions

This paper proposes a two-stage stochastic optimization problem to manage charging loads and co-optimize the provision of energy arbitrage and frequency regulation services from a BEV-charging station.

The model considers DERs, such as solar PV and BES. We use an SAA approach to efficiently solve the problem and can use the model in a rolling-horizon fashion to control a charging station in real-time.

We demonstrate the model using a case study of a public dc fast charging station that is co-located with a commercial retailer in Central Ohio. We examine the performance of the model and charging station in a number of sensitivity cases. We demonstrate that the model is able to use the available flexibility from BEVs and BES to provide high-quality and responsive frequency regulation. Our sensitivity analyses show that the ability of the charging station to provide frequency regulation is closely tied to the availability of BES and the size of the BEV-charging loads. It can provide frequency regulation in the absence of BES by exploiting the flexibility in BEV charging, however. The power capacity of BEV chargers can impact transformer loading, however the size of BEV-charging loads has a much greater impact. An asymmetric frequency regulation signal has some small impacts on the ability of the station to provide frequency regulation, with a negative bias being beneficial.

Many grid services, including frequency regulation, are transacted day ahead. However, real-time adjustments to the provision of these services can be made. We focus on such real-time provision of these services. Doing so allows the charging station to fully utilize the flexibility that is afforded by BEV recharging. Otherwise, if one focuses solely on providing grid services day ahead, the charging station is severely limited in only being able to make decisions based on its day-ahead assessment of how much BEV-charging flexibility it will have.

Our case study shows that the provision of grid services, including frequency regulation, generates significant value. As noted before, this value stream can be divided between BEV and charging-station owners. In doing so, the two parties are incentivized to adopt BEVs (in favor of conventional vehicles) and build public BEV-charging stations, respectively. There is, however, an important issue of how to contract to divide these benefits, which our work does not explore. As part of this contracting, BEV owners must be provided with incentives to provide flexibility in having their vehicle batteries recharged. A number of works, including those of Wu et al. (2012); Sioshansi (2012); Ma et al. (2013); Xi and Sioshansi (2014); Latinopoulos et al. (2017), examine the use of decentralized price-based mechanisms for co-ordinating BEV charging. These works assume that there is no centralized entity that directly controls and co-optimizes the charging of BEVs. Rather, charging decisions are left to individual BEV owners. However, various dynamic pricing schemes are developed in these works to incentivize BEV owners to charge their vehicles at times that are beneficial from an overall system perspective. As such, these works could represent one method of attaining the co-ordination that our model requires. Indeed, Donadee and Ilić (2014) build on this concept by developing a methodology to optimize the strategies that are employed by BEV owners to offer frequency regulation services into a market.

Another 'agency' issue that we do not examine is the relationship between the charging-station operator and the transformer owner. Distribution transformers are normally owned, maintained, and replaced by the local distribution utility, which may not be the owner of the charging station. Thus, implementing our proposed model, which allows the transformer to be overloaded, may require some form of contracting arrangement between those two parties. Namely, the utility must allow the charging station operator to overload the transformer, in exchange for sharing the increased cost of infrastructure replacement, which is necessitated by the resulting accelerated transformer aging. We do not explore how such arrangements might be structured. However, private communications with a number of distribution utilities reveal an interest in the concept that we propose here. More specifically, these utilities recognize that it is costly to resize distribution transformers to accommodate the anticipated load peak of public charging stations (especially in light of their relatively low capacity factors). Thus, they are interested in developing analytical capacities to balance accelerated transformer aging with the cost of undertaking a transformer replacement. Our model does such a balancing, insomuch as objective function (2) captures the financial tradeoff between overloading the distribution transformer and providing BEV-charging and grid services. Absent such contracting, the model formulation would have to be adjusted to exclude the possibility of overloading the distribution transformer. This can be done by fixing v_j and $v_{t,\omega}$ to zero. Hu et al. (2014); Aravinthan and Jewell (2015); Shao et al. (2017) also develop co-ordination models to ensure that BEV charging does not create such transmission- or distribution-level overloads. These contracting questions (*i.e.*, between BEV and charging-station owners and between charging-station owners and utilities) are important topics for further study.

Another issue that we do not examine here is the 'net value' of providing these services to the system. Although using BEV-charging flexibility to provide frequency regulation generates market revenue, there are important and non-trivial infrastructure and implementation costs. Chargers would need the physical capability to control and modulate the rate at which BEVs are charged. Moreover, charging stations would need on-site or cloud-based computational resources. Finally, robust two-way communications between BEV-charging stations and power system operators would be needed. These necessary systems all entail costs, analysis of which is beyond the scope of our work. Another important implementation question is how to make BEV-charging control robust to intermittent loss of communication or computation, which may be an issue in this type of setting. To our knowledge, the type of charging control that we envision here is not yet implemented in a commercial setting. Rather, most charging-control pilot projects are more focused on managing BEV charging to minimize retail costs (*e.g.*, demand-charge management). We believe that once the industry is more comfortable with these more formative forms of charging control, it will eventually evolve toward the provision of services that we study in this paper.

Acknowledgments

The authors thank Armin Sorooshian, the editors, and two reviewers for helpful discussions and suggestions. The material in this paper is based upon work that was financially supported by the United States Department of Energy under Award Number DE-PI0000012 and by the National Science Foundation through Grant Number 1029337. This work was also supported by an allocation of computing time from the Ohio Supercomputer Center. Any opinions and conclusions expressed in this paper are solely those of the authors.

References

Amini, M. H., McNamara, P., Weng, P., Karabasoglu, O., Xu, Y., December 2018. Hierarchical Electric Vehicle Charging Aggregator Strategy Using Dantzig-Wolfe Decomposition. IEEE Design & Test 35, 25–36.

Aravinthan, V., Jewell, W., March 2015. Controlled Electric Vehicle Charging for Mitigating Impacts on Distribution Assets. IEEE Transactions on Smart Grid 6, 999–1009.

Arsie, I., Marano, V., Rizzo, G., Moran, M., 18 August 2009. Integration of Wind Turbines with Compressed Air Energy Storage. In: Power Control and Optimization: Proceedings of the Second Global Conference on Power Control and Optimization. Vol. 1159. American Institute of Physics, pp. 11–18.

Bayraksan, G., Morton, D. P., September 2006. Assessing solution quality in stochastic programs. Mathematical Programming 108, 495–514.

Bayraksan, G., Morton, D. P., July-August 2011. A Sequential Sampling Procedure for Stochastic Programming. Operations Research 59, 898–913.

Bessa, R. J., Matos, M. A., April 2012. Economic and technical management of an aggregation agent for electric vehicles: a literature survey. European Transactions on Electrical Power 22, 334–350.

Cai, H., Jia, X., Chiu, A. S. F., Hu, X., Xu, M., December 2014. Siting public electric vehicle charging stations in Beijing using big-data informed travel patterns of the taxi fleet. Transportation Research Part D: Transport and Environment 33, 39–46.

Cao, Y., Wang, T., Kaiwartya, O., Min, G., Ahmad, N., Abdullah, A. H., April 2018. An EV Charging Management System Concerning Drivers' Trip Duration and Mobility Uncertainty. IEEE Transactions on Systems, Man, and Cybernetics: Systems 48, 596–607.

Dallinger, D., Krampe, D., Wietschel, M., June 2011. Vehicle-to-Grid Regulation Reserves Based on a Dynamic Simulation of Mobility Behavior. IEEE Transactions on Smart Grid 2, 302–313.

Denholm, P., Letendre, S. E., September 2007. Grid Services From Plug-In Hybrid Electric Vehicles: A Key to Economic Viability? In: Electrical Energy Storage—Applications and Technology Conference.

Dobos, A. P., September 2014. PVWatts Version 5 Manual. Tech. Rep. NREL/TP-6A20-62641, National Renewable Energy Laboratory, Golden, CO.

Donadee, J., Ilić, M. D., March 2014. Stochastic Optimization of Grid to Vehicle Frequency Regulation Capacity Bids. IEEE Transactions on Smart Grid 5, 1061–1069.

Dong, X., Mu, Y., Jia, H., Wu, J., Yu, X., October 2016. Planning of Fast EV Charging Stations on a Round Freeway. IEEE Transactions on Sustainable Energy 7, 1452–1461.

Drury, E., Denholm, P., Sioshansi, R., August 2011. The Value of Compressed Air Energy Storage in Energy and Reserve Markets. Energy 36, 4959–4973.

Fetene, G. M., Hirte, G., Kaplan, S., Prato, C. G., Tscharaktschiew, S., June 2016. The economics of workplace charging. Transportation Research Part B: Methodological 88, 93–118.

Frade, I., Anabela, R., Goncalves, G., Antunes, A. P., 2011. Optimal Location of Charging Stations for Electric Vehicles in a Neighborhood in Lisbon, Portugal. Transportation Research Record: Journal of the Transportation Research Board 2252, 91–98.

Gong, Q., Midlam-Mohler, S., Marano, V., Rizzoni, G., 25-26 May 2011. PEV Charging Impact on Residential Distribution Transformer Life. In: 2011 IEEE Energytech. Institute of Electrical and Electronics Engineers, Cleveland, OH, United States.

He, F., Wu, D., Yin, Y., Guan, Y., January 2013. Optimal deployment of public charging stations for plug-in hybrid electric vehicles. Transportation Research Part B: Methodological 47, 87–101.

He, F., Yin, Y., Zhou, J., November 2015. Deploying public charging stations for electric vehicles on urban road networks. Transportation Research Part C: Emerging Technologies 60, 227–240.

Hodgson, M. J., July 1990. A Flow-Capturing Location-Allocation Model. Geographical Analysis 22, 270–279.

Hu, J., You, S., Lind, M., Østergaard, J., March 2014. Coordinated Charging of Electric Vehicles for Congestion Prevention in the Distribution Grid. IEEE Transactions on Smart Grid 5, 703–711.

Janjic, A., Velimirovic, L., Stankovic, M., Petrusic, A., June 2017. Commercial electric vehicle fleet scheduling for secondary frequency control. Electric Power Systems Research 147, 31–41.

Kempton, W., Letendre, S. E., September 1997. Electric Vehicles as a New Power Source for Electric Utilities. Transportation Research Part D: Transport and Environment 2, 157–175.

Kempton, W., Tomić, J., 1 June 2005a. Vehicle-to-grid power fundamentals: Calculating capacity and net revenue. Journal of Power Sources 144, 268–279.

Kempton, W., Tomić, J., 1 June 2005b. Vehicle-to-grid power implementation: From stabilizing the grid to supporting large-scale renewable energy. Journal of Power Sources 144, 280–294.

Kuby, M., Lim, S., June 2005. The flow-refueling location problem for alternative-fuel vehicles. Socio-Economic Planning Sciences 39, 125–154.

Latinopoulos, C., Sivakumar, A., Polak, J. W., July 2017. Response of electric vehicle drivers to dynamic pricing of parking and charging services: Risky choice in early reservations. Transportation Research Part C: Emerging Technologies 80, 175–189.

Li, S., Huang, Y., Mason, S. J., April 2016. A multi-period optimization model for the deployment of public electric vehicle charging stations on network. Transportation Research Part C: Emerging Technologies 65, 128–143.

Ma, Z., Callaway, D. S., Hiskens, I. A., January 2013. Decentralized Charging Control of Large Populations of Plug-in Electric Vehicles. IEEE Transactions on Control Systems Technology 21, 67–78.

Pantoš, M., May 2012. Exploitation of Electric-Drive Vehicles in Electricity Markets. IEEE Transactions on Power Systems 27, 682–694.

Rebours, Y. G., Kirschen, D. S., Trotignon, M., Rossignol, S., February 2007a. A Survey of Frequency and Voltage Control Ancillary Services—Part I: Technical Features. IEEE Transactions on Power Systems 22, 350–357.

Rebours, Y. G., Kirschen, D. S., Trotignon, M., Rossignol, S., February 2007b. A Survey of Frequency and Voltage Control Ancillary Services—Part II: Economic Features. IEEE Transactions on Power Systems 22, 358–366.

Sener, I. N., Ferdous, N., Bhat, C. R., Reeder, P., October 2009. Tour-Based Model Development for TxDOT: Evaluation and Transition Steps. Tech. Rep. FHWA/TX-10/0-6210-2, Center for Transportation Research at The University of Texas at Austin, Austin, Texas.

Sengupta, M., Habte, A., Gotseff, P., Weekley, A., Lopez, A., Anderberg, M., Molling, C., Heidinger, A., September 2014a. A Physics-Based GOES Product for Use in NREL's National Solar Radiation Database. Tech. Rep. NREL/CP-5D00-62776, National Renewable Energy Laboratory, Golden, CO.

Sengupta, M., Habte, A., Gotseff, P., Weekley, A., Lopez, A., Molling, C., Heidinger, A., July 2014b. A Physics-Based GOES Satellite Product for Use in NREL's National Solar Radiation Database. Tech. Rep. NREL/CP-5D00-62237, National Renewable Energy Laboratory, Golden, CO.

Shahraki, N., Cai, H., Turkay, M., Xu, M., December 2015. Optimal locations of electric public charging stations using real world vehicle travel patterns. Transportation Research Part D: Transport and Environment 41, 165–176.

Shao, C., Wang, X., Shahidehpour, M., Wang, X., Wang, B., January 2017. Partial Decomposition for Distributed Electric Vehicle Charging Control Considering Electric Power Grid Congestion. IEEE Transactions on Smart Grid 8, 75–83.

Shapiro, A., Dentcheva, D., Ruszczyński, A., 2014. Lectures on Stochastic Programming: Modeling and Theory, 2nd Edition. Society for Industrial and Applied Mathematics, Philadelphia, Pennsylvania.

Shi, Q., Zheng, X., July 2014. Electric Vehicle Charging Stations Optimal Location Based on Fuzzy C-means Clustering. Applied Mechanics and Materials 556-562, 3972–3975.

Sioshansi, R., May-June 2012. Modeling the Impacts of Electricity Tariffs on Plug-in Hybrid Electric Vehicle Charging, Costs, and Emissions. Operations Research 60, 506–516.

Sioshansi, R., Denholm, P., 2010. The Value of Plug-In Hybrid Electric Vehicles as Grid Resources. The Energy Journal 31, 1–23.

Sioshansi, R., Denholm, P., Jenkin, T., Weiss, J., March 2009. Estimating the Value of Electricity Storage in PJM: Arbitrage and Some Welfare Effects. Energy Economics 31, 269–277.

Uddin, K., Jackson, T., Widanage, W. D., Chouchelamane, G., Jennings, P. A., Marco, J., 15 August 2017. On the possibility of extending the lifetime of lithium-ion batteries through optimal V2G facilitated by an integrated vehicle and smart-grid system. Energy 133, 710–722.

Upchurch, C., Kuby, M., November 2010. Comparing the p-median and flow-refueling models for locating alternative-fuel stations. Journal of Transport Geography 18, 750–758.

Upchurch, C., Kuby, M., Lim, S., January 2009. A Model for Location of Capacitated Alternative-Fuel Stations. Geographical Analysis 41, 85–106.

Wang, Y.-W., Lin, C.-C., September 2009. Locating road-vehicle refueling stations. Transportation Research Part E: Logistics

and Transportation Review 45, 821–829.
Wang, Y.-W., Wang, C.-R., September 2010. Locating passenger vehicle refueling stations. Transportation Research Part E: Logistics and Transportation Review 46, 791–801.
Wenzel, G., Negrete-Pincetic, M., Olivares, D. E., MacDonald, J., Callaway, D. S., September 2018. Real-Time Charging Strategies for an Electric Vehicle Aggregator to Provide Ancillary Services. IEEE Transactions on Smart Grid 9, 5141–5151.
Wu, C., Mohsenian-Rad, H., Huang, J., March 2012. Vehicle-to-Aggregator Interaction Game. IEEE Transactions on Smart Grid 3, 434–442.
Wu, F., Sioshansi, R., June 2017a. A Stochastic Flow-Capturing Model to Optimize the Location of Fast-Charging Stations with Uncertain Electric Vehicle Flows. Transportation Research Part D: Transport and Environment 53, 354–376.
Wu, F., Sioshansi, R., August 2017b. A Two-Stage Stochastic Optimization Model for Scheduling Electric Vehicle Charging Loads to Relieve Distribution-System Constraints. Transportation Research Part B: Methodological 102, 55–82.
Xi, X., Sioshansi, R., May 2014. Using Price-Based Signals to Control Plug-in Electric Vehicle Fleet Charging. IEEE Transactions on Smart Grid 5, 1451–1464.
Xi, X., Sioshansi, R., January 2016a. A Dynamic Programming Model of Energy Storage and Transformer Deployments to Relieve Distribution Constraints. Computational Management Science 13, 119–146.
Xi, X., Sioshansi, R., 2016b. Quantifying the Energy-Storage Benefits of Controlled Plug-in Electric Vehicle Charging. International Journal of Energy and Power 5, 26–34.
Xi, X., Sioshansi, R., Marano, V., July 2013. Simulation-optimization model for location of a public electric vehicle charging infrastructure. Transportation Research Part D: Transport and Environment 22, 60–69.
Xi, X., Sioshansi, R., Marano, V., September 2014. A Stochastic Dynamic Programming Model for Co-optimization of Distributed Energy Storage. Energy Systems 5, 475–505.
Xu, B., Shi, Y., Kirschen, D. S., Zhang, B., November 2018. Optimal Battery Participation in Frequency Regulation Markets. IEEE Transactions on Power Systems 33, 6715–6725.
Yan, Q., Zhang, B., Kezunovic, M., 2018. Optimized Operational Cost Reduction for an EV Charging Station Integrated with Battery Energy Storage and PV generation. IEEE Transactions on Smart GridIn press.